Novel Chirped Multilayer Quantum-Dot Lasers

G. Lin*[a], C. Y. Chang[a], W. C. Tseng[a], C. P. Lee[a], K. F. Lin[b], R. Xuan[b], and J. Y. Chi[c]
[a]Dept. of Electronics Engineering, National Chiao-Tung Univ., Hsinchu, 30010, Taiwan, R.O.C;
[b]Electronics and Optoelectronics Research Laboratories, ITRI, Hsinchu, 31040, Taiwan, R.O.C.
[c]Inst. of Opto-Electronic Engineering, National Dong-Hwa Univ., Hualien, 97401, Taiwan, R.O.C.

ABSTRACT

Chirped multilayer ($N=10$) QD lasers with 2-, 3- and 5-layer of longer-, medium-, and shorter-wavelength QD stacks, respectively, were grown in this work. Low threshold current density and high saturated modal gain were achieved in this specially designed QD structure. Empirical gain-current analysis was performed on this chirped multilayer QD structure for the first time. It was consistent with our spectral observations and provided valuable information on carrier recombination in chirped multilayer QD structure. Two novel spectral characteristics were discovered also for the first time. First, simultaneous two-wavelength lasing around threshold was observed under particular gain-loss condition at this specific multilayer structure of QD stacking numbers. Second, at cryogenic temperature, simultaneous two-wavelength lasing emissions switched from longer-wavelength lasing first to shorter-wavelength lasing first with increasing current injection. Non-uniform carrier distribution among chirped multilayer QD structure is evident at low temperature below 200 K from our analysis.

Keywords: quantum dots, semiconductor lasers, molecular beam epitaxy, spectral characteristics, temperature characteristics, gain-current characteristics, chirped multilayer QDs, optical coherent tomography.

1. INTRODUCTION

Self-assembled growth of semiconductor quantum dots (QDs) is subjected to inhomogeneity in shapes, sizes and compositional non-uniformity, which result in lower saturated optical gain. Multilayer QD structure by stacking multiple QD layers of same growth condition (or uniform-stacked) is incorporated to increase the optical gain for high performance QD lasers of long-wavelength range [1]. Nonetheless, the intrinsic spectral characteristics of non-homogeneous broadening in QDs, if properly engineered, are promising for low optical coherence applications such as optical fiber communications, fiber-optic gyroscopes, and optical coherence tomography. Recently, mature QD growth technology has enabled stacking multiple QD layers of different emission wavelengths (or chirp-stacked) for semiconductor broadband light emitters [2, 3].

Of the special interest is the broad spectral emission superluminescent light emitting diodes (SLEDs) based on gain medium of InAs QDs grown on low-cost GaAs substrates [2]. By operating the diode in the superluminescent mode (stimulated emission without optical feedback), net optical gain is preserved but without coherent oscillation. The spectral narrowing in lasing emission is therefore inhibited, and amplified spontaneous emission with broad spectral emission is then achieved. However, lower output power in SLEDs may limit its performance on real-time image scanning. Moreover, the tilted ridge waveguide (RW) configuration for low mirror reflectivity complicates the fiber-waveguide coupling and increases the package cost. It was announced very recently that QD lasers, in normal RW configuration, can be managed to lase with a very wide emission spectrum [3, 4]. The higher power characteristics of diode lasers are of course the best candidate to broadband light emitters.

SLEDs based on chirped multilayer QD active region were achieved with certain success; however, systematic studies on chirped QD lasers are limited for their low saturated gain and complex lasing spectra. In this work, we have demonstrated 10-layer QD lasers with three chirped-wavelength QD-stacks. Novel spectral characteristics are for the first time observed and discussed. Empirical analysis on device optical gain is also discussed in this investigation. It provides valuable information for designing broadband light emitters or even advanced semiconductor light sources.

*graylin@mail.nctu.edu.tw; phone +886-3-5131289; fax +886-3-5724361

2. DEVICE GROWTH AND FABRICATION

The QD laser structure was grown by molecular beam epitaxy on n^+-GaAs (100) substrate. The InAs QDs were self-assembled in the Stranski-Krastanow (S-K) growth mode. When the QDs are covered by an InGaAs strain-reducing layer (SRL), a red-shift of the emission wavelength can be achieved [2]. To chirp the emission wavelengths, we have intentionally varied the thickness of InGaAs SRL at nominal In composition of 0.15 so that the growth parameters could be easily reproducible and well-controlled.

Multilayer QD active region with undoped step-index separate-confinement heterostructure (step-SCH) of 0.5 μm was sandwiched between Si-doped and C-doped $Al_{0.35}Ga_{0.65}As$ cladding layers of 1.5 μm, and followed by heavily C-doped GaAs contact layer of 0.4 μm. The emission wavelengths of InAs QDs are tuning by the subsequent $In_{0.15}Ga_{0.85}As$ capping layer of different thickness. Multilayer QDs are spaced by GaAs and centered in the active region also by GaAs. The spacing thickness of 33 nm is chosen so that strain is not accumulated in the multilayer deposition.

To chirp the emission wavelengths of QD active region, three wavelengths designated as QD_L, QD_M and QD_S (stand for longer-, medium- and shorter-wavelength QD stacks, respectively) were engineered in the laser structure, which corresponding to the InAs QDs of 2.6 ML capped by InGaAs of 4 nm, 3 nm and 1 nm, respectively. The stacking numbers for QD_L, QD_M and QD_S were 2, 3 and 5 layers, respectively. The stacking sequence was arranged so that QD_L was near the n-side. Fig. 1 shows the schematic diagram of chirped multilayer QD structure.

Standard RW was processed by wet etching and subsequent dielectric lift-off. The etching depth was carefully monitored to stop 200 nm above the active region. After p-metallization by Ti/Pt/Au deposition, the substrate was thin down to around 100 μm, and n-type metal of AuGe/Ni/Au was deposited afterwards. As-cleaved laser bars with cavity lengths from 0.4 mm to 5 mm were then evaluated by standard light-current-voltage (L-I-V) and spectrum measurement. Both pulsed and continuous-wave driving conditions are performed under varied heatsink temperature.
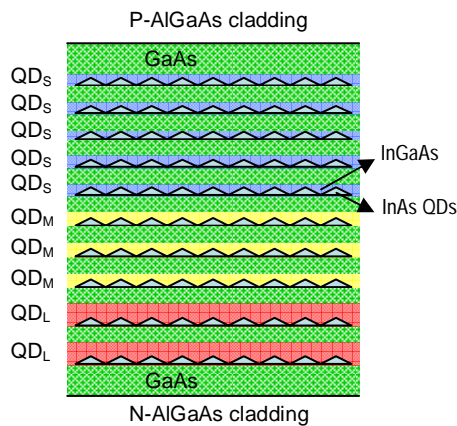

Fig. 1. The schematic diagram of chirped multilayer QD structure.

3. RESULTS AND DISCUSSION

The areal density of InAs QDs without InGaAs capping was grown separately and characterized by AFM to be around $5*10^{10}$ cm^{-2}. Since the QD areal density is not significantly affected by the capping, the available gain and the spectral range are effectively increased by stacking chirped multiple InAs QD layers in which each QD layer is covered with different InGaAs SRL [2]. The dependence of peak emission wavelength of a single QD layer as a function of the thickness of $In_{0.15}Ga_{0.85}As$ SRL can be determined from room-temperature (RT) photoluminescence (PL). Referring to the work by L. H. Li et al [2], the peak emission wavelengths of ground state (GS) for QD_L, QD_M and QD_S in our case were about 1262 nm, 1230 nm, and 1175 nm, respectively. The peak emission wavelengths of first excited state (ES) for QD_L, QD_M and QD_S were also estimated to be around 1183 nm, 1155 nm, and 1107 nm, respectively.

In this section, the L-I-V and spectral characteristics of semiconductor lasers was presented. Then the laser parameters of internal loss and internal quantum efficiency were extracted. Finally, the gain-current analysis with empirical fitting was

for the first time performed on this chirped multilayer QD structure. The lasing wavelengths as well as their origin of QD stacks were identified from the analysis.

3.1 Laser Characteristics

Fig. 2 shows the RT pulsed *L-I-V* characteristics of chirped QD lasers in narrow RW of 5 μm with different cavity lengths. The lasing spectra around threshold relevant to different cavity lengths are shown in Fig. 3. Longer lasing wavelength around 1262 nm was achieved for cavity lengths above 2 mm, while shorter lasing wavelength of 1133 nm was measured for cavity length below 0.4 mm. The lasing emissions covered a huge spectral range of about 130 nm in single epitaxial structure. The medium lasing wavelength range (1185 nm ~ 1215 nm) was for cavity lengths in between. Simultaneous two-wavelength lasing at 1261 nm and 1215 nm around threshold was observed for the cavity length of 2 mm. The current injection was as low as 30 mA or 60 A/cm^2/per-QD if both two-layer longer-wavelength QD-stack (designates as 2*QD$_L$) and three-layer medium-wavelength QD-stack (designated as 3*QD$_M$) are considered to have the equal contribution to the lasing emission. This is believed to be the first observation of simultaneous two-wavelength lasing from two GS at such lower current density. For the cavity length of 5 mm, the current threshold was 100 A/cm^2 or 50 A/cm^2/per-QD if only 2*QD$_L$ contributed to the lasing emission.
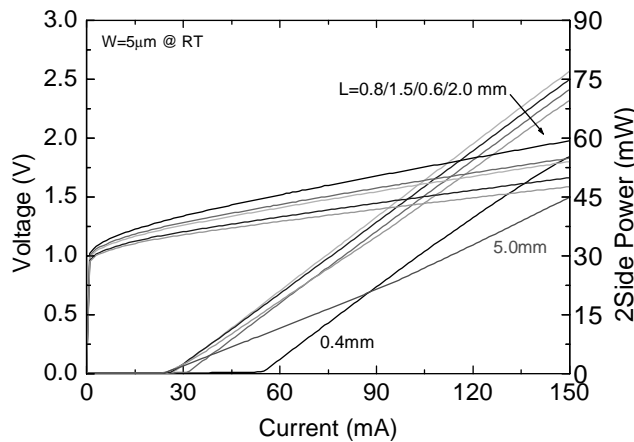
Fig. 2. The RT *L-I-V* characteristics of chirped multiple QD lasers for different cavity lengths.
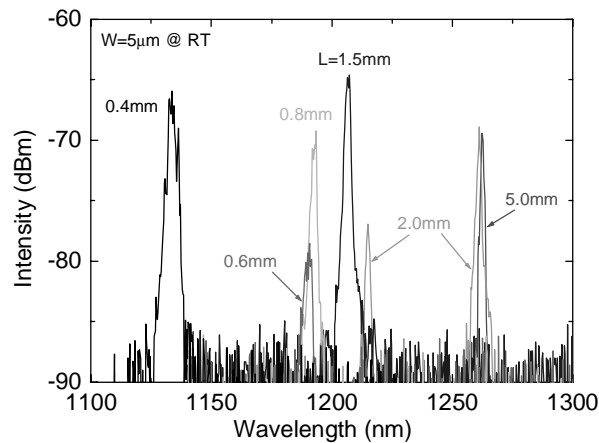
Fig. 3. The RT lasing spectra of chirped multiple QD lasers operating around threshold for different cavity lengths.

To further characterize the chirped QD laser structure, we have made the dependence plot of threshold current density versus inverse cavity length (shown in Fig. 4) as well as inverse external quantum efficiency versus cavity length (shown in Fig. 5). The estimated threshold current density at infinite cavity length is almost zero. The extracted internal quantum efficiency is almost 100 % while the internal loss is about 4.7 cm^{-1}. To mention, internal loss around 5 cm^{-1} is not uncommon in the narrow ridge waveguide configuration. The excellent epitaxy growth and device fabrication are therefore manifested from our analysis.
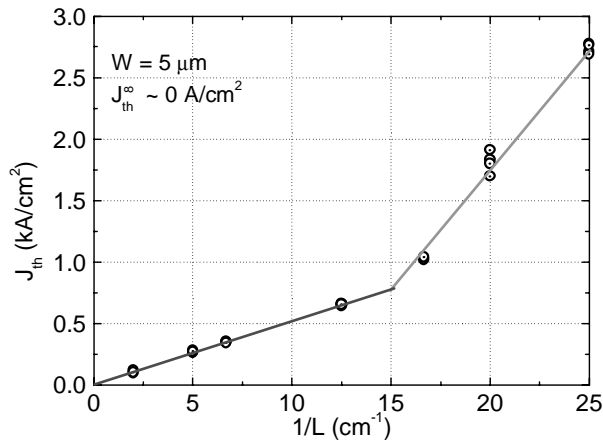

Fig. 4. Threshold current density plotted as a function of cavity length of chirped multilayer QD lasers.
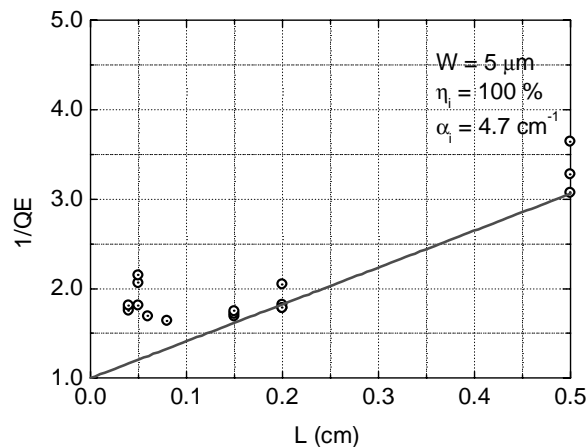

Fig. 5. Inverse of external differential efficiency plotted as a function of cavity length of chirped multilayer QD lasers.

3.2 Gain-Current Analysis

The dependence of the gain on current density is one of the main characteristics of the active medium in an injection laser, closely related to the electronic structure of the active region. We experimentally determined the current dependence of threshold modal gain (*g-J*) for studying the multilayer structure of real QD arrays. Since real QDs are suffered from inhomogeneous broadening with lower saturated gain, the *g-J* curve is departed from the usual logarithmic dependence of QW gain medium. We have therefore fitted the gain curve based on the empirical equation proposed by Zhukov et al. [6], i.e.

$$g = g^{sat}\left[1 - \exp\left(-\gamma\frac{J - J_0}{J_0}\right)\right] \tag{1}$$

where J_0 is the transparency current and γ-factor is an additional gain parameter related to the linear gain region. The fitting parameters of ground-state saturated gain per-QD layer and γ-factor are fixed for all QD layers of chirped multilayer structure as they were grown at the same conditions, however, the current densities to make transparent the three chirped QD stacks of different InGaAs capping thickness are different for the three chirped wavelengths. The experimental data points and fitting curves are shown in Fig. 6. The lasing wavelengths at each threshold condition were also shown for the sake of analysis.

Since the lasing wavelengths switched significantly at cavity lengths of 2 mm and 0.4 mm, a first approximation should reveal two different saturated values of optical gain (or total optical loss) around 10.4 cm^{-1} and 33.2 cm^{-1}. Further analysis using the fitting procedures mentioned above resolved two values of 10.4 cm^{-1} and 28.0 cm^{-1}, corresponding to GS and ES emissions, respectively, from 2*QD$_L$. The GS saturated gain per QD is then 5.2 cm^{-1}, which fits very well in the reasonable range of 4~6 cm^{-1}. The level degeneracies of QD are first approximated by the ratio of ES-to-GS saturated gain to be 2.69, which also fits very well in the range of 2-3 [7, 8]. The GS saturated gains for 3*QD$_M$ and 5*QD$_S$ are therefore determined to be 15.6 cm^{-1} and 26 cm^{-1}, respectively, while the ES saturated gains for 3*QD$_M$ and 5*QD$_S$ are 42 cm^{-1} and 70 cm^{-1}, respectively. Worth to mention, total dot densities and level degeneracies are taken into consideration in determining the transparency current densities.
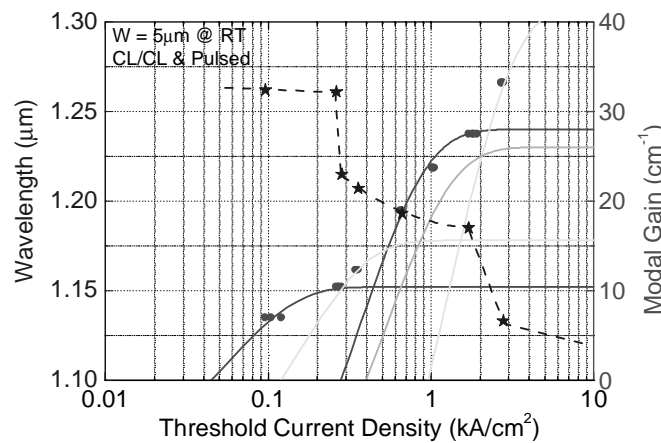

Fig. 6. Modal gain and lasing wavelength as functions of current densities of chirped multilayer QD lasers.

3.3 Spectral Characteristics

In Fig. 2, we have observed simultaneous two-wavelength lasing from GS of both QD$_L$ and QD$_M$ at low injection current of 30mA, which means that the carrier population among 2*QD$_L$ and 3*QD$_M$ results in the equal contribution of threshold modal gain at these two wavelengths. The argument is consistent with our analysis in Fig. 6 through the crossing of two gain curves. This observation is very different from simultaneous GS and ES lasing emissions from conventional uniform-stacked multilayer QD active region [5], wherein incomplete gain claming and the retarded carrier relaxation process in QD are the main attribution. We can infer from the above analysis that around threshold, simultaneous two-wavelength lasing emissions from ES of QD$_L$ and GS of QD$_M$ as well as those from ES of both QD$_L$ and QD$_M$ are also possible to be observed with proper cleavage of cavity lengths.

The wavelength range from 1185 nm to 1215 nm around lasing threshold for cavity lengths between 0.5 mm and 2 mm was attributed to the GS of QD$_M$ and / or first ES of QD$_L$. Lasing emission from GS of QD$_S$ cannot be observed around threshold throughout all cavity lengths. However, as current pumped well above threshold, stimulated emissions from

different QD stacks that surpass the total optical loss do contribute the measured spectra as if they are lasing independently from different QD ensembles. Fig. 7 shows the RT lasing spectra operating from lasing threshold to well-above threshold for laser device with 5μm in ridge width and 0.6mm in cavity length. The GS emission spectrum evolved from ES of QD_M, then to GS of QD_S, and finally to ES of QD_M.
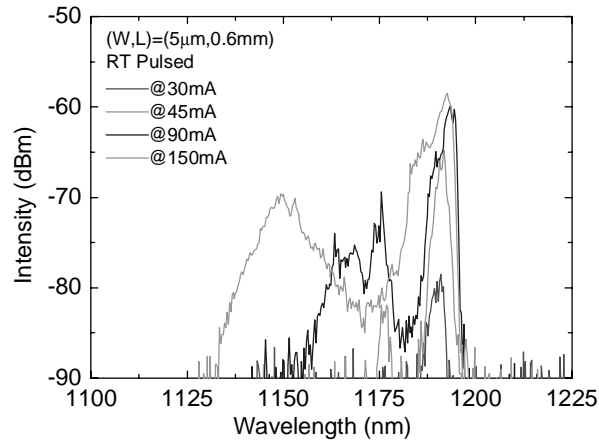

Fig. 7. The RT lasing spectra operating from lasing threshold to well-above threshold for chirped multilayer QD laser with 5μm in ridge width and 0.6mm in cavity length.

The lasing wavelength of 1133 nm for cavity length of 0.4 mm deviated from our prediction at first ES of QD_M around 1155 nm. Significant band filling with increasing current injection along with the carrier population over high energy state at elevated junction temperature may play the dominant role.

3.4 Temperature Characteristics

To get further information of this novel chirped multilayer QD structure, we have carried out the temperature varying measurement of TO-packaged QD lasers. The device under test was 50 μm in ridge width and 3 mm in cavity length. Fig. 8 shows the temperature-dependent *L-I-V* characteristics and associated current-dependent lasing spectra at two nominal temperatures of 100 K and 220 K. With decreasing temperature, the threshold current decreased to a minimum of 50 mA (or 25 A/cm^2/per-QD) at nominal temperature of 240 K, and then increased monotonically to have negative characteristic temperature. The current-dependent spectral measurements revealed simultaneous two-wavelength lasing with longer-then-shorter wavelength in the initial temperature ramping down; however, we have observed for the first time the anomalous shorter-then-longer lasing emissions with increasing current injection at ambient temperature below 200 K.

At nominal temperature of 100 K, the emission spectra around threshold showed the enhanced carrier population among 3*QD_M for higher optical gain or intensified optical output at shorter wavelength. Kinks in L-I around threshold with sharp increase were accompanied with the observation as a result of absorption bleaching among 2*QD_L. We have therefore confirmed the non-uniform carrier distribution in this chirped multilayer QD lasers. Negative characteristic temperature in multilayer QD lasers, which is believed to be indication of non-Fermi carrier statistics among different-sized QD [6], is also observed in our chirped multilayer QD structure. Our direct evidence of non-uniform carrier distribution among multilayer QD worsened the non-equilibrium process and exhibited itself with very poor characteristic temperature.
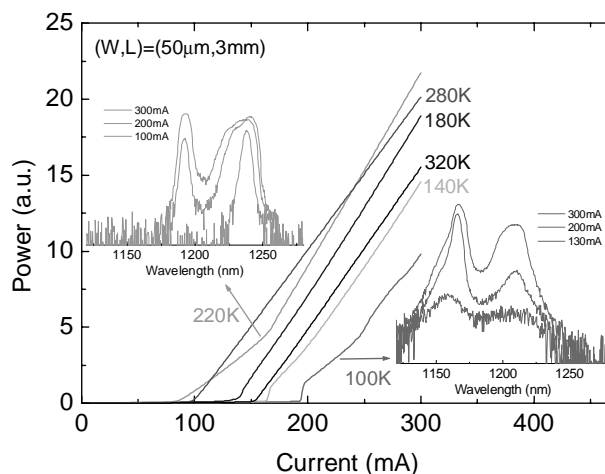
Fig. 8. The temperature-dependent *L-I-V* of chirped multilayer QD laser and associated current-dependent lasing spectra

4. CONCLUSIONS

In summary, we have demonstrated the multilayer (*N=10*) QD lasers with 2-, 3-, amd 5-layer of longer-, medium, and shorter-wavelength QD states, respectively. Low threshold current density and high saturated modal gain were achieved even in this specially designed QD structure. The lasing wavelength around 1260 nm, 1215 nm and 1135 nm were observed and identified to ground states and / or excited states of different chirped-wavelength QD-stacks. Analysis of gain-current characteristics for chirped multilayer QD structure was performed for the first time and consistent with our spectral observations. Two novel spectral characteristics were discovered also for the first time in our investigation. First, simultaneous two-wavelength lasing around threshold was observed under particular gain-loss condition at this specific multilayer structure of QD stacking numbers. Second, with increasing current injection above threshold, simultaneous two-wavelength lasing emissions switched from longer-wavelength first to shorter-wavelength first at cryogenic temperature. The lasing spectra at even higher current injection, with broader emission spectra, were still under extensive study and will be reported elsewhere. Further investigation and optimization of chirped QD structure may lead to novel light emitters and diverse applications in optical communication as well as biomedical imaging and diagnostics.

5. ACKNOWLEDGMENT

REFERENCES

[1]   G. Lin , I. F. Chen, F. J. Lay and J. Y. Chi, D. A. Livshits, A. R. Kovsh and V. M. Ustinov, "High-performance ridge-waveguid multi-stack (N = 2, 5, and 10) InAs/InGaAs/GaAs quantum dot lasers of 1.3 um range," Intl. J. Nanosci. 3(1&2), 187-192 (2004).
[2]   L. H. Li, M. Rossetti, A. Fiore, L. Occhi and C. Velez, "Wide emission spectrum from superluminescent diodes with chirped quantum dot multilayers," Electron. Lett. 41(1), 41-43 (2005).

[3] H. S. Djie, B. S. Ooi, X.-M. Fang, Y. Wu, J. M. Fastenau, and W. K. Liu, "Room-temperature broadband emission of an InGaAs/GaAs quantum dots laser," Opt. Lett. 32(1), 44-46 (2007).

[4] Innolume GmbH, "NL Nanosemiconductor announces Broad Band Lasers based on Quantum Dot Technology," http://www.innolume.com/news_060607.htm (2006).

[5] A. Markus, J. X. Chen, C. Paranthoen, A. Fiore, C. Platz, and O. Gauthier-Lafaye, "Simultaneous two-state Lasing in quantum-dot lasers," Appl. Phys. Lett. 82(12), 1818-1820 (2003).

[6] A. E. Zhukov, V. M. Ustinov, A. Y. Egorov, A. R. Kovsh, A. F. Tsataulnikov, N. N. Ledentsov, S. V. Zaitsev, N. Y. Gor-deev, P. S. Kopev, and Z. I. Alferov, "Negative characteristics temperature of InGaAs quantum dot injection laser," Jpn. J. Appl. Phys. 36(6B), 4216-4218 (1997).

[7] A E Zhukov, A R Kovsh, V M Ustinov, A Yu Egorov, N N Ledentsov, A F Tsatsul'nikov, M V Maximov, Yu M Shernyakov, VIKopchatov, A V Lunev, PSKop'ev, D Bimberg and Zh I Alferov, "Gain characteristics of quantum dot injection lasers," Semicond. Sci. Technol. 14, 118-123 (1999).

[8] G. Park, O. B. Shchekin, and D. G. Deppe, "Temperature Dependence of Gain Saturation in Multilevel Quantum Dot Lasers," IEEE J. Quantum Electron. 36(9), 1065-1071 (2000).